ROYAL SOCIETY
OF CHEMISTRY

PAPER

Check for updates

Novel delivery system: a liquid crystal emulsion containing HSO crystals†

Lin Ding,[a] Hanglin Li,[a] Zhicheng Ye,[a] Yazhuo Shang, (iD) *[a] Xiong Wang*[b] and Honglai Liu[a]

Oil-in-water (O/W) emulsions with lamellar liquid crystal interfaces are promising drug-delivery systems for topical formulations. In this study, a novel delivery system—an O/W liquid crystal emulsion system containing an oil crystal network—was constructed by introducing a fully hydrogenated soybean oil (HSO) to a liquid crystal emulsion, and then the properties of the system were studied in detail. The results showed that with the introduction of the HSO, the Maltese cross patterns of the liquid crystal interface became brighter and subtle crystals of HSO gradually appeared in the inner of the liquid crystal texture. The aliphatic acid and triacylglycerols (TAGs) in HSO participated in the orderly arrangement of the lamellar interfacial phase, which not only benefited the formation of liquid crystals and recovery of the interfacial dynamic equilibrium at higher temperature but also endowed the system with a stronger interfacial film and better thermal stability. The aliphatic acid and TAGs recrystallized inside the emulsion droplets, forming a crystal network inside the droplets. The combination of HSO crystals and liquid crystals increased the characteristic temperature (T_c) of the liquid crystals and decreased the HSO melting point, which benefited the display performance of the liquid crystal emulsion and the effective application of the HSO. At the same time, the formation of both a strengthened interfacial film of liquid crystal and three-dimensional HSO crystal network inside the droplets made the emulsion system show better storage stability, mechanical strength, and deformation resistance. Furthermore, the unique structure of the liquid crystal emulsion containing HSO crystals endowed the system with an excellent sustainable release property and potential application prospects in medicine, personal care, and other fields. The present study not only provides an effective delivery system but also expands the application potential of HSO and liquid crystal emulsion systems in practice.

1. Introduction

Controlled drug-delivery systems (DDSs) can achieve better drug efficacy through the release of a drug at a specific site as well as the sustained release of the drug, and thus have become advanced methods for the transport of drugs, due to the fact that they can overcome the limitations of traditional drug formulations.[1,2] Lyotropic liquid crystal systems (LLCs) are one of the most promising candidates for DDSs. As a self-assembled mesophase, lyotropic liquid crystals exhibit a unique structure that is in between an ordered solid phase and true liquid phase.[3] LLCs are usually composed of amphiphilic molecules that can spontaneously form long-range ordered structures under certain environments. LLCs exhibit various phase behaviors, including lamellar, hexagonal, and cubic phases, at different conditions[4,5] The ordered structure formed by amphiphilic materials provide LLCs passageways for the controlled release of various components.[6,7] LLCs have been widely used in pharmaceutical fields, such as drug stability, disorder treatment, and skin care.[2,8,9] Various types of liquid crystal carriers have been investigated, including hydrogels, microemulsions, and injectable formulations.[7,9,10] Liquid crystal emulsions are a new type of system with emulsifier molecules arranged orderly at the interface between oil and water, forming a lamellar liquid crystal structure. The existence of a liquid crystal structure endows the emulsion system with better stability, slower release, and better moisturizing properties, as well as sensory properties, than ordinary emulsions.[11] Liquid crystal emulsions have shown excellent application prospects in skin care in recent years. The lamellar liquid crystal has a similar structure to the stratum corneum and has a higher affinity with human epidermis, which can strengthen the effective recovery of the barrier function.[11,12]

[a] *Key Laboratory for Advanced Materials, School of Chemistry & Molecular Engineering, East China University of Science and Technology, Shanghai 200237, China. E-mail: shangyazhuo@ecust.edu.cn*

[b] *Shanghai Sixth People's Hospital Affiliated to Shanghai Jiao Tong University School of Medicine, Shanghai 200233, China. E-mail: xiongw89@sina.com*

† Electronic supplementary information (ESI) available. See DOI: https://doi.org/10.1039/d3nj01050c

This journal is © The Royal Society of Chemistry and the Centre National de la Recherche Scientifique 2023

However, studies on the property and application of liquid crystal emulsions are relatively scarce. Developing an effective functional delivery system for skin care based on a liquid crystal emulsion and exploration of its potential application are still necessary. Fully hydrogenated soybean oil (HSO) is a low-cost hydrogenation product with a specific melting and crystal behavior, composed of stearic acid and triacylglycerols (TAGs).[13] With a content of 85 wt% stearic acid, hydrogenated soybean oil has no adverse effects on the cardiovascular disease risk.[13,14] Recent studies have shown that the crystals of the oil play an important role in controlled delivery systems.[15,16] In binary oil/fat mixtures, growing needle-like crystal formations would provide a 3D solid network.[17] Disordered crystalline fibers in the oil matrix can allow a satisfactory encapsulation of drugs.[15,18,19] Moreover, the solid–liquid phase transitions of oil crystals will also impact the formation, thermal stability, and sustained drug release of emulsion-based delivery systems.[15] Solid oils also play a key role in the rheological and sensory characteristics of systems.[20] However, The presence of crystals in the droplets can cause aggregation in traditional O/W emulsions.[21] It was also found that particles consisting of hydrogenated soybean oil would experience melting behaviors and coalescence issues during storage.[22] It is difficult to disperse and stabilize high-melting point fats, like hydrogenated soybean oil. We speculated that if we were to introduce HSO to a liquid crystal emulsion, the system may have brilliant properties and the corresponding disadvantages should potentially be solved.

Consequently, in this work, a liquid crystal emulsion system containing HSO crystals was constructed by introducing HSO to a lamellar liquid crystal emulsion system based on hydrogenated lecithin. The properties of the created system were studied by polarized light microscopy, X-ray diffraction (XRD), and differential scanning calorimetry (DSC), as well as rheological measurements. The in vitro release behavior of the studied system was also explored using vitamin E as the detecting object. The results can provide guidance not only for the design and preparation of novel liquid crystal delivery systems but also for the effective applications of HSO in practice.

2. Material and methods

2.1. Materials

A liquid crystal emulsifier containing hydrogenated lecithin was developed by our laboratory (fatty acid < 2 wt%). Hydrogenated lecithin (S-10) was obtained from Nikkol Chemicals Co., Ltd (Japan). HSO (fully hydrogenated, ~85 wt% stearic acid) was obtained from Yihan Kerry Foodstuffs Marketing CO., Ltd (China). Caprylic/capric triglyceride (GTCC) was obtained from BASF (Germany). Ethanol (C_2H_5OH) was purchased from Shanghai Aladdin Biochemical Technology Co., Ltd (China). Vitamin E was obtained from Beijing Brilliance BIOTECH Co., Ltd (China). Carbopol U21 was obtained from Lubrizol Special Chemical Co., Ltd (America). Sodium hydroxide (NaOH) was purchased from Shanghai Titan Polytron Technologies Inc (China). Ultrapure water with a resistivity of 18.2 MΩ cm obtained from a Millipore Simplicity water purification system was used for all the experiments. All the chemicals were used without further purification.

2.2. Preparation of liquid crystal emulsions

The liquid crystal emulsifier, GTCC, and HSO were mixed as an oil phase in a beaker at 80 ± 0.5 °C. Ultrapure water with Carbopol U21 was added into another beaker as the water phase at the same temperature of 80 °C. Then, the oil phase was added into the water phase under homogenization using an homogenizer (T25 digital, IKA, Germany) at 6000 revolutions per minute (rpm) for approximately 7 min. The emulsion was then stirred in a blender (UROSTAR 60 Control, IKA, Germany) at 25 ± 0.5 °C to cool down for 30 min. During the cooling process, the sodium hydroxide solution was added gradually to adjust the pH value to neutrality. The emulsion samples were cooled to 25 ± 0.5 °C, and then bottled and stabilized for 24 h. The liquid crystal emulsions were obtained and the corresponding compositions are shown in Table 1. For the samples used in the release tests, we added vitamin E into the oil phase (the concentration of vitamin E was 5%, samples 6 and 7).

2.3. Evaluation of the structures and properties of the liquid crystal emulsion

2.3.1. Optical microscopy. The microstructures and birefringence of the samples were photographed by a Nikon polarizing microscope (50iPOL; Nikon, Japan), under both bright-field and polarized light. Fresh emulsion was placed in a 25 ± 0.5 °C incubator (PH 050A; Yiheng, China) for 24 h. Then, a small amount of emulsion was applied on a glass slide with a cover glass at 25 ± 0.5 °C for observation. Images were analyzed using Image J software (ImageJ, Maryland, USA).

2.3.2. X-Ray diffraction (XRD) measurement. X-Ray diffraction (XRD) measurements were performed under the condition of Cu Kα radiation wavelength (λ = 0.1541 nm), with an X-ray diffractometer (D/max-2550 VB/PC; Rigaku, Japan). The spacing

Table 1 Compositions of the liquid crystal emulsions

Sample	Emulsifier/wt%	HSO/wt%	GTCC/wt%	Vitamin E/wt%	Carbopol U21/wt%	NaOH/wt%	Water/wt%
1	5.0	0.0	12.0	0.0	0.1	0.2	Up to 100
2	5.0	4.8	7.2	0.0	0.1	0.2	Up to 100
3	5.0	7.2	4.8	0.0	0.1	0.2	Up to 100
4	5.0	9.6	2.4	0.0	0.1	0.2	Up to 100
5	5.0	12.0	0.0	0.0	0.1	0.2	Up to 100
6	5.0	0.0	12.0	5.0	0.1	0.2	Up to 100
7	5.0	9.6	2.4	5.0	0.1	0.2	Up to 100

values were calculated by Bragg's equation (according to the XRD patterns).

2.3.3. DSC measurements. HSO, the liquid crystal emulsion without HSO, and the liquid crystal emulsion with HSO crystals were measured by differential scanning calorimetry DSC25 (Netzsch, America). HSO was held in a pure aluminum crucible, while the emulsions were sealed in the crucible. The weight of the sample in every test was 5 mg. The samples were kept at 25 °C and then heated at a heating rate of 5 °C min^{-1} to 80 °C, and then cooled from 80 °C to 25 °C at a cooling rate of −5 °C min^{-1} within ± 0.5 °C accuracy, with a flow rate of 50 mL min^{-1} N$_2$.

2.3.4. Rheological measurements. The rheological properties of the liquid crystal emulsion were measured using a cone plate system (CP50-1) with a radius of 50 mm and a taper angle of 1° for the physical MCR 302 rheometer (Anton Paar; Gratz, Austria).

The flow sweep was performed at 25 ± 0.5 °C by changing the shear rates from 0.01 to 1000 s^{-1}. The obtained data were fitted with the Herschel–Bulkley model, as shown in eqn (1).

$$\tau = \tau_{HB} + K\gamma^n \tag{1}$$

where τ is the shear stress (Pa), τ_{HB} is the yield stress (Pa), γ is the shear rate (s^{-1}), K is the flow coefficient (Pa s^n), and n is the flow behavior index. When n was less than 1, it indicated that the system was a non-Newtonian pseudoplastic fluid. For the thixotropy test, the flow curves of the emulsions were obtained at 25 ± 0.5 °C by increasing the shear rate from 0.01 to 1000 s^{-1} and decreased from 1000 to 0.01 s^{-1} after pausing for 1 s. The oscillatory amplitude sweep test was performed by applying strain from 0.001% to 100% with a frequency of 1 Hz at 25 ± 0.5 °C, and the linear viscoelastic range (LVR) was calculated (5% deviation in the linearity of the storage modulus G'). Tests with the variation of the modulus at different temperatures were conducted at a strain of 0.1% and a frequency of 1 Hz, heating the emulsion samples from 25 ± 0.5 °C to 55 ± 0.5 °C at a heating speed of 5 °C min^{-1}.

2.3.5. *In vitro* release studies. The dialysis method was used to study the release behavior of the liquid crystal emulsion. We used ethanol as the release medium, and loaded approximately 1.0 g of sample in a dialysis bag (molecular weight cutoff of 3500 Da). The dialysis bag was suspended in 100 mL release medium and shaken in a thermostatic shaker at 37 ± 0.5 °C with a stirring speed of 100 rpm. At predetermined time intervals, 5 mL of release medium was taken and measured with an ultraviolet spectrophotometer (UV-2450; Shimadzu, Japan) at a wavelength of 284.5 nm to calculate the vitamin E concentration. Meanwhile, the same volume of blank medium was added to maintain a constant volume.

Using the ultraviolet regression equation of vitamin E in alcohol (as shown in Fig. S1, ESI†), we detected the concentration of vitamin E in the extracted medium. Then, the cumulative release ratio (CRR) of vitamin E was calculated by the following formula:

$$CRR(\%) = \left(\frac{C_t V_0 + \sum_{0}^{t-1} C_t V_t}{m} \right) \times 100\% \tag{2}$$

where C_t is the concentration measured at time t, respectively, V_0 is the volume of the release medium (100 mL), V_t is the volume taken out each time (5 mL), and m is the mass of vitamin E in the sample. Each experiment was repeated at least three times. The data collected from the *in vitro* release experiments were analyzed with the software SPSS (IBM SPSS Statistics 26). Statistical significance between each group was assessed by one-way ANOVA The significance thresholds were considered significant ($P < 0.05$), highly significant ($P < 0.01$), or extremely significant ($P < 0.001$).

2.3.6 Stability tests. The emulsion samples were divided into two groups. One group was placed in a 45 ± 0.5 °C incubator (PH 050A; Yiheng, China) for 30 days to test the high-temperature stability of the emulsion. The other group was placed in a 25 ± 0.5 °C incubator (PH 050A; Yiheng, China) for 6 months to examine the long-term storage stability of the emulsion.

3. Results and discussion

3.1. Microstructure

Polarizing microscopy is usually used to examine the solid crystal and liquid crystal textures. Fig. 1 presents the polarizing microscopic images for different systems. It can be seen that HSO presented a bright needle-like structure even in GTCC (Fig. 1(f)). The typical "cruciate flower" texture, namely Maltese cross patterns, was observed in the liquid crystal emulsion without HSO (Fig. 1(a)).[1,23] With the introduction of HSO, subtle crystals appeared in the inner Maltese cross patterns (Fig. 1(b)–(e)), which should be attributed to the homogeneous nucleation of TAGs molecules in HSO.[19,24] Furthermore, the Maltese crosses become brighter compared with the system
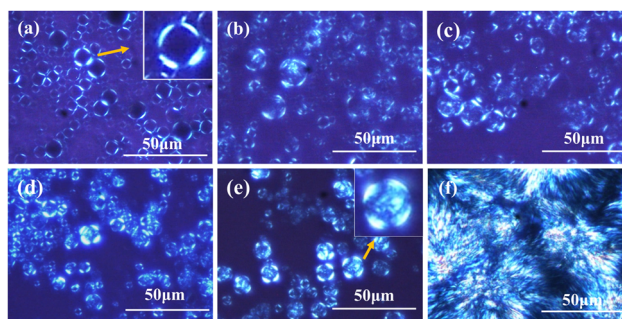
Fig. 1 Polarizing microscopic images: (a) liquid crystal emulsion without HSO; (b) liquid crystal emulsion with 4.8 wt% HSO; (c) liquid crystal emulsion with 7.2 wt% HSO; (d) liquid crystal emulsion with 9.6 wt% HSO; (e) liquid crystal emulsion with 12.0 wt% HSO; (f) HSO crystal in GTCC, m (GTCC : HSO) = 5 : 1.

without HSO. Obviously, the aliphatic chains of the introduced HSO could align and be gathered at the oil–water interfaces, which could enhance the ordered arrangement of interfacial active species at the droplet interface.[25,26] The existence of the produced irregular crystal had an adverse effect on the formation of perfect spherical droplets to a certain degree (see Fig. S2, ESI†).[20] Obviously, the introduced HSO not only crystallized in the oily interior but could also participate in the formation of the liquid crystal texture of the droplet interface.

During the experiments, we found that the dispersion of the emulsion droplets became more and more uniform with the increase in HSO concentration, which improved the stability of the emulsion (in Fig. S3, ESI†).

3.2. X-Ray diffraction (XRD) measurements

X-Ray diffraction (XRD) is a very suitable technique for identifying polymorphs since each polymorph has its own characteristic diffraction pattern.[27] Fig. 2 shows the XRD patterns of HSO and the liquid crystal emulsion containing HSO, respectively.

Pure HSO presented multiple peaks in the range of 15°–30° in 2θ, which refers to the polymorphic forms of aliphatic acid and TAGs. Some of these peaks were found in the emulsion, indicating the formation of HSO crystals in the droplets. The obtained spacing values, namely hydrogen bond distances (3.85 Å and 4.23 Å), indicated the formation of TAGs in the β' form and aliphatic acids in the studied system.[27,28] The results reconfirmed the formation of a crystal structure in the emulsion sample. The crystallization of bulk oil followed a heterogeneous nucleation pathway, while oil in the droplets showed an homogeneous nucleation.[29] Obviously, HSO went through a different crystallization inside the emulsion droplet compared to its bulk phase during the cooling process. The aliphatic chain rearranged in the droplet core should be the reason for the difference in the XRD patterns. The difference in nucleation

Fig. 2 XRD patterns (d-spacing values 3.0–6.0 Å) of pure HSO and the liquid crystal emulsion with HSO crystals.

and growth inside the droplet would contribute to the regulation of the crystallization kinetics.[29]

3.3. Thermal behavior of the liquid crystal emulsion

DSC measurements were performed to investigate the thermal behaviors of the liquid crystal emulsions. Moisture evaporation of the emulsions occurred during the whole test, resulting in sloping curves. The liquid crystal emulsion without HSO showed an endothermic melting at 41.4 °C (Fig. 3(a)), corresponding to the characteristic temperature (T_c) of the lamellar phases.[1] The order/disorder transition of hydrocarbon chains happens above the T_c, changing the lamellar structure from an ordered or gel state to a disordered or liquid-like state.[30] When HSO was introduced into the liquid crystal emulsion, the T_c of the lamellar structure increased to about 45.8 °C, which may be attributed to the participation of TAGs in the formation of the bilayer hydrophobic microregions. The existence of HSO in the lamellar phase benefited the species at the interface forming a more orderly arrangement even at higher temperature, which endowed the system containing HSO with better thermal stability.

The melting of pure HSO and HSO in the liquid crystal emulsion system occurred almost over the same temperature range (from about 38.8 °C to 59.3 °C), which also verified the crystalline state of HSO in the droplets.[29] Meanwhile, HSO in the liquid crystal system showed a decrease in the endothermic peak temperature (51.1 °C and 45.8 °C for pure HSO and HSO in the liquid crystal system, respectively). This may be due to the participation of HSO for the bilayer formation, and correspondingly, the disorder transitions of both the liquid crystal and HSO crystal happened at about 45 °C simultaneously (as confirmed in Fig. 3(c)). The decrease in melting point of HSO in the liquid crystal emulsion facilitates the usage of HSO and provides a guidance for the practical application of high-melting-point oil.

As for cooling process, shown in Fig. 3(b), the liquid crystal emulsion showed a flat peak, corresponding to the recovery of the orderly structure at the interface. The liquid crystal structure at the oil–water interface gradually formed during cooling (showed in Fig. S4, ESI†).[31] The liquid crystals were formed at 39.1 °C and 42.7 °C for the liquid crystal emulsion without HSO and with HSO, respectively. The participation of HSO for the formation of lamellar interfacial phase benefited the orderly arrangement of species in the lamellar phase and further promoted the recovery of the interfacial dynamic equilibrium even at higher temperature.

Furthermore, it was found (in Fig. 3) that the liquid crystal without HSO was destroyed at a temperature of 41.4 °C and then recovered at a temperature of 39.1 °C reversibly. Whereas with the introduction of HSO, the liquid crystal would not be destroyed until 45.8 °C and could self-recover at higher temperature (42.6 °C). Obviously, the system containing HSO showing better thermal stability. All of these should be attributed to the participation of aliphatic acids and TAGs in HSO in the formation of the lamellar interfacial phase. The combination of the liquid crystal and HSO crystal thus could create a
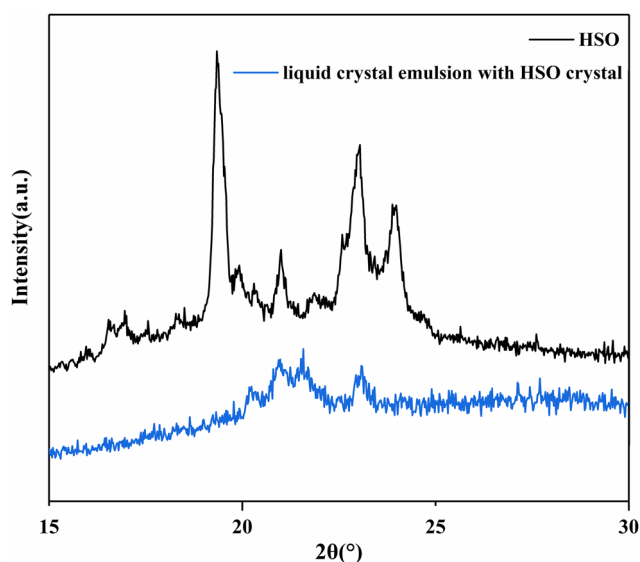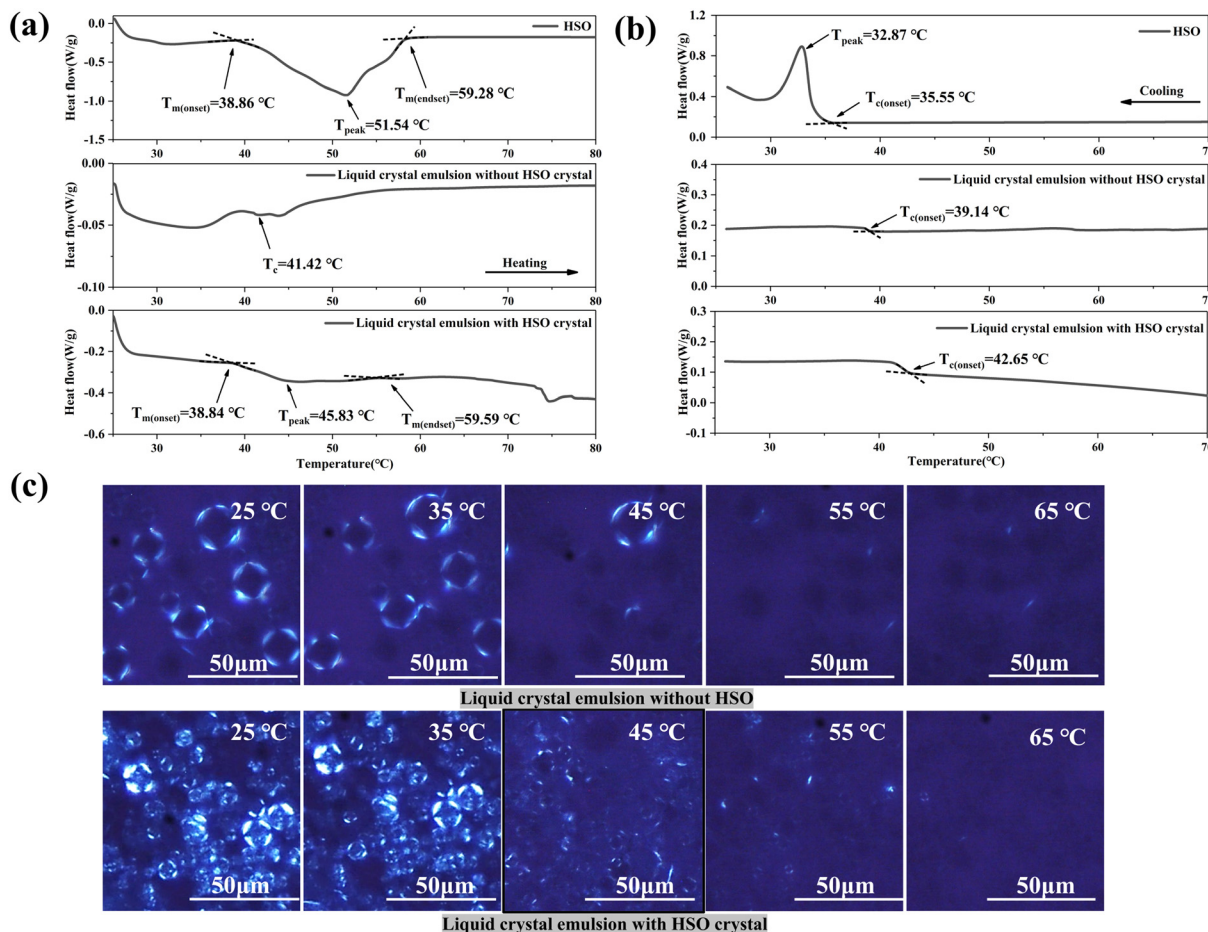
Fig. 3 (a) DSC heating scan of emulsions with and without HSO crystals from 25 °C to 80 °C at a heating speed of 5 °C min^{-1}; (b) DSC cooling scans of the emulsions with and without HSO crystals from 80 °C to 25 °C at a cooling speed of −5 °C min^{-1}. (c) Polarizing microscopic images of the liquid crystal emulsions under 25 °C to 65 °C.

more exploitable and thermally stable system, which may broaden the practical application of both liquid crystal systems and high-melting-point oil.

3.4. Rheological properties of the liquid crystal emulsion

3.4.1. Shear-thinning behavior and thixotropy. The underlying microstructure of an emulsion confers a macroscopic flow property to the system.[32] In order to explore the effect of HSO crystal on the liquid crystal emulsion, the rheological properties of the system were studied. Just as with traditional emulsions, the emulsion system with and without HSO showed a typical shear-thinning behavior (Fig. 4(a)).[33] The rheology behavior of the emulsion was analyzed by fitting the data with the Herschel–Bulkley model, as shown in Table 2.

The results showed that the liquid crystal emulsion without HSO had a yield value of 2.80 Pa, and K values of 6.84 Pa s^n, representing a great storage stability and spreadability during application. Both the yield values and K value increased with the HSO concentration for the studied system (when the system contained 9.6% HSO, the yield stress and K value of the system reached 7.06 Pa and 11.99 Pa s^n, respectively), which indicated
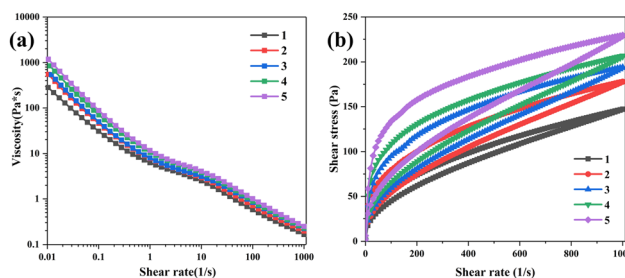

Fig. 4 Rheological properties of emulsions containing HSO with different concentrations. (a) Steady-shear viscosity curves at shear rates from 0.01 to 1000 s^{-1}; (b) thixotropy curves at shear rates from 0.01 to 1000 s^{-1} and decreasing from 1000 to 0.01 s^{-1} after pausing for 1 s.

higher initial stress was required to produce flow, thus indicating the stronger network structure for the system containing more HSO.[34] Meanwhile, the thixotropic curve showed a clockwise hysteresis loop, manifesting the existence of a recoverable network structure composed of the liquid crystals in the studied system.[31] The thixotropic breakdown coefficient (K_d) produced better results in the comparative investigations of the

Table 2 Flow parameters (fitted by the Herschel–Bulkley equation) and K_d of the liquid crystal emulsions

HSO (wt%)	τ_{HB} (Pa)	K (Pa s^n)	n	R^2	K_d
0.0	2.81	6.84	0.46	1.0000	0.278 ± 0.014
4.8	4.54	8.55	0.45	0.9999	0.355 ± 0.017
7.2	4.98	10.48	0.44	1.0000	0.477 ± 0.024
9.6	7.06	11.99	0.42	1.0000	0.468 ± 0.023
12.0	8.72	13.80	0.41	0.9999	0.520 ± 0.026

Data are presented as the mean $\pm$ standard deviation ($n = 3$).

Table 3 G_0', G_0'', LVR, and E_c values of the liquid crystal emulsions

HSO (%)	G_0' (Pa)	G_0'' (Pa)	LVR (%)	E_c (mJ m^{-3})
0.0	208.00 ± 10.00	38.99 ± 3.22	0.37 ± 0.003	1.41 ± 0.04
4.8	310.50 ± 12.03	48.44 ± 0.94	0.44 ± 0.06	3.49 ± 0.48
7.2	469.00 ± 6.53	56.86 ± 1.41	0.48 ± 0.07	4.31 ± 0.29
9.6	480.67 ± 1.89	51.63 ± 1.41	0.49 ± 0.002	5.65 ± 0.07
12.0	538.67 ± 18.37	57.21 ± 0.86	0.51 ± 0.02	7.09 ± 0.71

Data are presented as the mean $\pm$ standard deviation ($n = 3$).

systems, where the energy needed to destroy the structure of the system can be given by:[35,36]

$$K_d = (A_{up} - A_{down})/A_{up} \tag{3}$$

where A_{up} and A_{down} are the areas under the ascending and descending flow curves, respectively. In the present study, the K_d of the system increased with the HSO concentration, indicating that more energy was needed for disintegrating their structure, confirming the formation of stronger network structures in the system with HSO.[35,37]

Obviously, the addition of HSO enhanced the network structure and improved the storage stability of the system. Also, the rheological properties of the studied system, including the long-term storage, pumping, and spreading on a body could be tailored on purpose by adjusting the HSO concentration in practice.

3.4.2. Viscoelastic properties. Oscillatory amplitude sweep tests were used for revealing the viscoelastic property of the emulsions. As also shown in Fig. 5(a), the liquid crystal emulsion without HSO had a higher storage modulus (G') value than loss modulus (G'') in the linear viscoelastic region, exhibiting the characteristic of a gelled network.[20] With the introduction of HSO in the system, the G' values and G'' values increased. Compared to the G'' values, the responses of the G' values were dominant, indicating the enhancement of the elastic property of the system containing HSO.

Table 3 shows the linear viscoelastic region (LVR) and the cohesive energy (E_c) of the emulsions with different HSO concentrations. LVR is the linear portion of the storage modulus, and the cohesive energy can be calculated by eqn (4):[38]

$$E_c = \frac{1}{2}G_0'\gamma_c^2 \tag{4}$$

where E_c is the cohesive energy, G_0' is the storage modulus in the linear regime, and γ_c is the critical strain amplitude.

Both the linear viscoelastic region and the cohesive energy are important parameters for observing the strength of a system's structure.[38,39] The larger LVR of the liquid crystal emulsion containing HSO showed that a stronger network was formed. When the system contained 9.6% HSO, the E_c value was four times higher than that of the system without HSO, which also means that the system with HSO had a higher structural strength. Both of these results confirmed that the introduction of HSO strengthened the network structure in the emulsions, and the property of network structure could be tailored with the HSO concentration.

The effect of the HSO crystal on the viscoelasticity of the emulsion was examined by tracking the modulus of the system at different temperatures.[20] Here, emulsions were heated from 25 °C to 55 °C at a heating speed of 5 °C min^{-1}. As shown in Fig. 5(b), the liquid crystal emulsion without HSO had lower modulus values and these showed no obvious changes with the rise in temperature. The water in the liquid crystal structure gradually evaporated, resulting in a minor increase in the modulus values. Meanwhile, the values of both G' and G'' decreased above a temperature of about 40 °C for the emulsions containing HSO. This should be derived from the destruction of the three-dimensional HSO crystal network inside the droplets. The modulus of the emulsion decreased continually with the increase in temperature and kept almost constant until about 50 °C, which was related to the melting of the HSO crystal. It is clear that the viscoelastic properties of the emulsion strongly depended on the formation of HSO crystals. Both the enhanced interfacial film of the liquid crystal and the formation of the HSO crystal network in liquid crystal droplets improved the mechanical strength and deformation resistance of the emulsion.

3.5. *In vitro* release studies

Topical formulations containing vitamin E are effective skin care products for stabilizing the skin barrier.[40] Vitamin E can prevent photocarcinogenesis induced by UVB (290–320 nm) effectively, and resist exogenous free radicals significantly, which brings a possible salutary effect to reduce the cell damage caused by air pollution.[41,42] There are some commercially approved biopolymers for encapsulating vitamins, but the complex preparation process limits their application.[43]
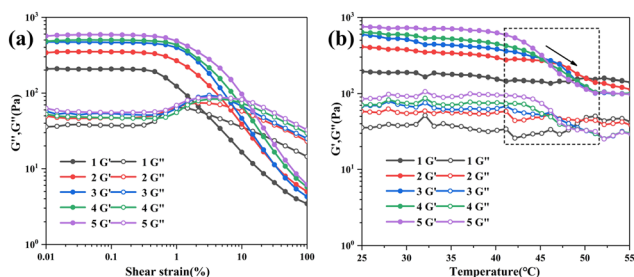
Fig. 5 Variation of G' and G'' of emulsions with different HSO concentration. (a) The strain scan from 0.01% to 100% at 25 °C; (b) the temperature scan from 25 ± 0.5 °C to 55 ± 0.5 °C at a heating speed of 5 °C min^{-1} with a strain of 0.1% and a frequency of 1 Hz.
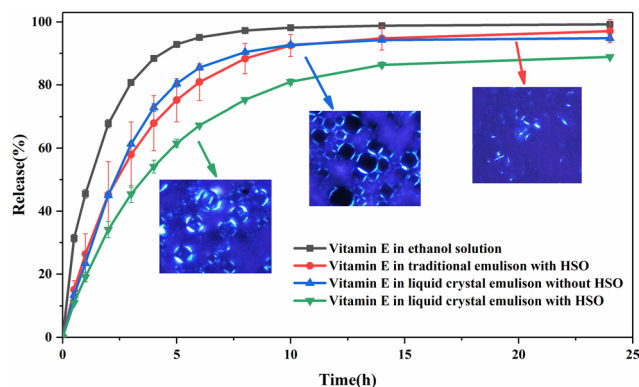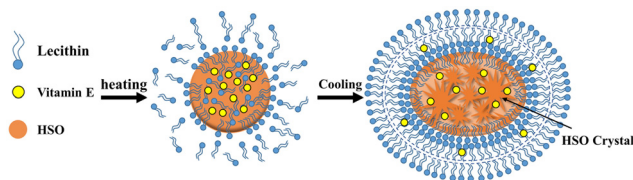
Fig. 6 Vitamin E *in vitro* release of different composition emulsions (ethanol solution, traditional emulsion with HSO, liquid crystal emulsion with and without HSO crystals) at $37 \pm 0.5\,°C$ for 24 h. Data are presented as the mean $\pm$ standard deviation ($n = 3$).

It was confirmed that the chemical compositions, shapes, and other physicochemical properties of a system are crucial for their drug release property.[44] The physical state of the oil would change the migration of molecules in the emulsion droplet core.[45,46] Herein, vitamin E was introduced to a constructed liquid crystal emulsion containing HSO crystals and the corresponding release properties were further explored. The release property of the system was explored by measuring the 24 h cumulative release amount of vitamin E at $37 \pm 0.5\,°C$. As shown in Fig. 6 and Fig. S5 (ESI†), the liquid crystal emulsion containing HSO showed significant release differences of vitamin E compared with the other samples after 2 h. The release of vitamin E in the liquid crystal emulsion with HSO crystals was only 34.17% after 2 h. While the cumulative release in ethanol solution, the traditional emulsion with HSO, and liquid crystal without HSO were 67.77%, 45.26%, and 45.09%, respectively. The time required for cumulative release to reach 50% ($T_{50\%}$) was used as a criterion for evaluating the release rate.[47] The $T_{50\%}$ in ethanol solution, the traditional emulsion with HSO, and liquid crystal emulsion with and without HSO crystal were 77.3, 144.18, 212.3, and 138.8 min, respectively. Clearly, either the liquid crystal or HSO crystal in the system had a sustainable release effect on vitamin E. The liquid crystal emulsion containing HSO crystals showed a more significant sustainable release behavior for vitamin E compared with the liquid crystal emulsion without HSO crystal and traditional emulsion containing HSO crystals.

As shown in Scheme 1, the possible mechanism for the formation of liquid crystal emulsions containing HSO crystals and their corresponding sustained release property is proposed. In the O/W emulsion system, most of the lipophilic ingredient will be trapped within the crystalline structure of the oil droplets.[29,48] Once the lamellar liquid crystal texture at the oil–water interface and the HSO crystal network inside the droplets are formed during the cooling process, most of the vitamin E will be encapsulated in the crystal network of HSO. On the one hand, the lamellar liquid crystal mesophase formed by lecithin provides hydrophobic domains to accommodate lipophilic ingredients, which helps achieving the sustainable release of loaded ingredients.[49,50] The participation of oil molecules can also benefit the species arrangement at the oil–water interface and strengthen the interfacial film.[51] On the other hand, the oil crystal network inside the droplets slows down the ingredient diffusion from the droplet core to the interface, limiting the release of lipophilic ingredients into the aqueous phase.[48,52] Here, the HSO crystal network formed inside the liquid crystal droplets restrained the transfer of vitamin E to a great degree. The combination of the strengthened lamellar liquid crystal at the oil–water interface and the HSO crystal network inside the droplet endowed the emulsion with excellent sustainable release property. Clearly, the release property of the unique structure could be tailored by adjusting the concentration of HSO.

3.6. Storage performance

It was found that the particle size of the liquid crystal emulsion without HSO increased after high-temperature storage (Fig. 7(a)). However, the liquid crystal emulsion containing HSO crystal could overcome the coalescence with longer storage at 45 °C, which showed its better high-temperature stability. Meanwhile, the liquid crystal emulsions were stored at 25 °C for 6 months. The liquid crystal emulsion containing HSO (9.6 wt%) remained uniform in appearance, while creaming occurred in the emulsion without HSO. The polarizing microscopic image in Fig. 7(b) showed that the morphologies of the emulsion droplets in the system developed in the present study had no obvious changes after 6 months of storage. That is, that the introduction of HSO effectively improved the storage stability of liquid crystal systems.

Scheme 1 Schematic illustration of the formation of the liquid crystal emulsion containing HSO crystal.
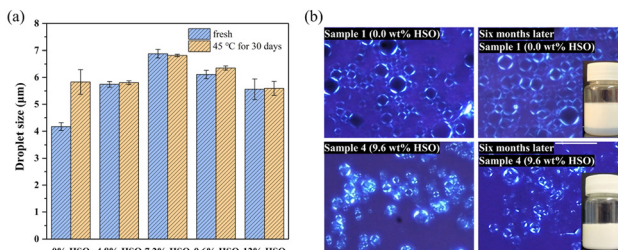

Fig. 7 (a) Droplet sizes of the liquid crystal emulsion before and after high-temperature tests. (b) Polarizing microscopic images of the emulsion after 6 months' storage.

This journal is © The Royal Society of Chemistry and the Centre National de la Recherche Scientifique 2023

4. Conclusions

In this study, we constructed a novel delivery system—O/W liquid crystal emulsion containing an oil crystal network—by introducing HSO to a liquid crystal emulsion. The results displayed that the introduced HSO brightened the Maltese cross patterns of the liquid crystal interface and formed a crystal network in the inner of the liquid crystal texture. The participation of aliphatic acid and TAGs in HSO for the liquid crystal interface formation not only benefited the recovery of the interfacial dynamic equilibrium at higher temperature but also endowed the system with a stronger interfacial film and better thermal stability. The effective combination of HSO crystal and the lamellar liquid crystal increased the characteristic temperature (T_c) of the liquid crystal and decreased the HSO melting point, which benefited the display performance of the liquid crystal emulsion and the application of HSO effectively. Furthermore, the coexistence of both a strengthened liquid crystal interfacial film and three-dimensional HSO crystal network inside the droplets endowed the emulsion system with better storage stability, mechanical strength, and deformation resistance. The constructed emulsion with a unique structure showed excellent sustainable release property and has potential application prospects in many fields, such as medicine, and personal care. The present work not only provides a delivery system with adjustable performance, but also provides necessary information for understanding the properties of liquid crystal/crystal combined emulsion systems and expands the application of HSO and liquid crystal emulsion systems.

Author contributions

Lin Ding: conceptualization, methodology, investigation, writing – original draft. Hanglin Li: conceptualization, methodology, investigation. Zhicheng Ye: methodology, investigation, validation. Yazhuo Shang: writing – review & editing, funding acquisition. Xiong Wang: methodology, validation. Honglai Liu: writing – review & editing.

Conflicts of interest

The authors declare no competing financial interests.

Acknowledgements

Notes and references

1 J. Hu, Z. Ni, H. Zhu, H. Li, Y. Chen, Y. Shang, D. Chen and H. Liu, *Int. J. Pharm.*, 2021, **607**, 121007.
2 D.-H. Kim, A. Jahn, S.-J. Cho, J. S. Kim, M.-H. Ki and D.-D. Kim, *J. Pharm. Invest.*, 2014, **45**, 1–11.
3 V. K. Rapalli, T. Waghule, N. Hans, A. Mahmood, S. Gorantla, S. K. Dubey and G. Singhvi, *J. Mol. Liq.*, 2020, **315**, 113771.
4 H. Wang, T. Peng, H. Wu, J. Chen, M. Chen, L. Mei, F. Li, W. Wang, C. Wu and X. Pan, *J. Controlled Release*, 2021, **338**, 623–632.
5 Y. Wang, R. M. F. Fernandes and E. F. Marques, *J. Mol. Liq.*, 2019, **285**, 330–337.
6 J. Fan, H. Zhang, M. Yi, F. Liu and Z. Wang, *J. Mol. Liq.*, 2019, **274**, 690–698.
7 Y. Li, A. Angelova, J. Liu, V. M. Garamus, N. Li, M. Drechsler, Y. Gong and A. Zou, *Colloids Surf., B*, 2019, **173**, 217–225.
8 H. K. Bisoyi and Q. Li, *Chem. Rev.*, 2022, **122**, 4887–4926.
9 C. M. Spillmann, J. Naciri, W. R. Algar, I. L. Medintz and J. B. Delehanty, *ACS Nano*, 2014, **8**, 6986–6997.
10 J. Yang, W. Cui, Y. Lu, B. Guan, X. Qiu and P. Liu, *J. Pet. Sci. Eng.*, 2015, **125**, 90–94.
11 Y. Wang, J. Li, Y. Shang and X. Zeng, *Colloids Surf., B*, 2018, **171**, 335–342.
12 J. F. De Souza, K. D. S. Pontes, T. F. R. Alves, V. A. Amaral, M. D. A. Rebelo, M. A. Hausen and M. V. Chaud, *Molecules*, 2017, **22**, 419.
13 A. P. B. Ribeiro, R. Grimaldi, L. A. Gioielli and L. A. G. Gonçalves, *Food Res. Int.*, 2009, **42**, 401–410.
14 J. E. Hunter, *Nutr. Res.*, 2005, **25**, 499–513.
15 D. J. McClements, *Adv. Colloid Interface Sci.*, 2012, **174**, 1–30.
16 J. N. Coupland, *Curr. Opin. Colloid Interface Sci.*, 2002, 7, 445–450.
17 T. S. Omonov, L. Bouzidi and S. S. Narine, *Chem. Phys. Lipids*, 2010, **163**, 728–740.
18 T. Wang and Y. Luo, *Nanoscale*, 2019, **11**, 11048–11063.
19 S. Ghosh and D. Rousseau, *Curr. Opin. Colloid Interface Sci.*, 2011, **16**, 421–431.
20 C. Liu, Z. Zheng, C. Xi and Y. Liu, *J. Colloid Interface Sci.*, 2021, **587**, 417–428.
21 K. Boode and P. Walstra, *Colloids Surf., A*, 1993, **81**, 121–137.
22 M. I. Landim Neves, M. de Souza Queirós, R. L. Soares Viriato, A. P. Badan Ribeiro and M. L. Gigante, *LWT – Food Sci. Technol.*, 2021, **152**, 112276.
23 C. C. Müller-Goymann, *Eur. J. Pharm. Biopharm.*, 2004, **58**, 343–356.
24 K. Boode, C. G. J. Bisperink and P. Walstra, *Colloids Surf.*, 1991, **61**, 55–74.
25 S. Ueno, Y. Hamada and K. Sato, *Cryst. Growth Des.*, 2003, **3**, 935–939.
26 S. Ali, A. Tiwari, T. Yeoh, P. Doshi, N. Kelkar, J. C. Shah and J. R. Seth, *Langmuir*, 2022, **38**, 8502–8512.
27 A. Langevelde, K. Malssen, F. Hollander, R. Peschar and H. Schenk, *Acta Crystallogr., Sect. B: Struct. Sci.*, 1999, **55**, 114–122.
28 V. Malta, G. Celotti, R. Zannetti and A. F. Martelli, *J. Chem. Soc. B*, 1971, 548–553.
29 L. Cornacchia and Y. H. Roos, *J. Food Sci.*, 2011, **76**, C1211–C1218.
30 G. Eccleston, *J. Soc. Cosmet. Chem.*, 1990, **41**, 1–22.
31 W. Zhang and L. Liu, *J. Cosmet., Dermatol. Sci. Appl.*, 2013, **03**, 139–144.

32 D. Bonn, M. M. Denn, L. Berthier, T. Divoux and S. Manneville, *Rev. Mod. Phys.*, 2017, **89**, 035005.

33 E.-K. Park and K.-W. Song, *Arch. Pharmacal Res.*, 2010, **33**, 141–150.

34 S. Tamburic, D. Q. M. Craig, G. Vuleta and J. Milic, *Int. J. Pharm.*, 1996, **137**, 243–248.

35 L. Lin, J. Huang, L. Zhao, J. Wang, Z. Wang and C. Wei, *Carbohydr. Polym.*, 2015, **134**, 448–457.

36 L. Dokić, T. Dapčević, V. Krstonošić, P. Dokić and M. Hadnađev, *Food Hydrocolloids*, 2010, **24**, 172–177.

37 X. Lu, R. Xu, J. Zhan, L. Chen, Z. Jin and Y. Tian, *Int. J. Biol. Macromol.*, 2020, **146**, 620–626.

38 T. F. Tadros, *Langmuir*, 1990, **6**, 28–35.

39 P. Pandey and G. D. Ewing, *Drug Dev. Ind. Pharm.*, 2009, **34**, 157–163.

40 J. J. Thiele and S. Ekanayake-Mudiyanselage, *Mol. Aspects Med.*, 2007, **28**, 646–667.

41 S. Krishnamurthy, *J. Chem. Educ.*, 1983, **60**, 465.

42 K. A. Kramer and D. C. Liebler, *Chem. Res. Toxicol.*, 1997, **10**, 219–224.

43 I. Katouzian and S. M. Jafari, *Trends Food Sci. Technol.*, 2016, **53**, 34–48.

44 Y. Zhang, F. Fang, L. Li and J. Zhang, *ACS Biomater. Sci. Eng.*, 2020, **6**, 4816–4833.

45 S. Okuda, D. J. McClements and E. A. Decker, *J. Agric. Food Chem.*, 2005, **53**, 9624–9628.

46 H. Bunjes and M. H. J. Koch, *J. Controlled Release*, 2005, **107**, 229–243.

47 H. Zhang and Z. Wang, *Int. J. Pharm.*, 2019, **565**, 283–293.

48 A. Gomes, A. L. R. Costa, P. J. D. A. Sobral and R. L. Cunha, *Food Hydrocolloids Health*, 2023, **3**, 100125.

49 H. Zhang, R. Hao, X. Ren, L. Yu, H. Yang and H. Yu, *RSC Adv.*, 2013, **3**, 22927–22930.

50 M. E. Carlotti, S. Sapino, M. Gallarate, M. Trotta, R. Cavalli, E. Ugazio and E. Peira, *J. Dispersion Sci. Technol.*, 2008, **29**, 1460–1470.

51 M. Douaire, V. di Bari, J. E. Norton, A. Sullo, P. Lillford and I. T. Norton, *Adv. Colloid Interface Sci.*, 2014, **203**, 1–10.

52 W. A. F. Wan Mohamad, D. McNaughton, M. A. Augustin and R. Buckow, *Food Chem.*, 2018, **257**, 361–367.